View Article Online / Journal Homepage / Table of Contents for this issue

Graphene, the new nanocarbon†

C. N. R. Rao,*[ab] Kanishka Biswas,[ab] K. S. Subrahmanyam[a] and A. Govindaraj[ab]

DOI: 10.1039/b815239j

Graphene is a fascinating new nanocarbon possessing, single-, bi- or few- (≤ ten) layers of carbon atoms forming six-membered rings. Different types of graphene have been investigated by X-ray diffraction, atomic force microscopy, transmission electron microscopy, scanning tunneling microscopy and Raman spectroscopy. The extraordinary electronic properties of single-and bi-layer graphenes are indeed most unique and unexpected. Other properties of graphene such as gas adsorption characteristics, magnetic and electrochemical properties and the effects of doping by electrons and holes are equally noteworthy. Interestingly, molecular charge-transfer also markedly affects the electronic structure and properties of graphene. Many aspects of graphene are yet to be explored, including synthetic strategies which can yield sufficient quantities of graphene with the desired number of layers.

Published on 20 January 2009. Downloaded by IIT Jodhpur on 11/2/2023 9:13:43 PM.

Introduction

Graphene is one of the most exciting materials being investigated today, not only out of academic curiosity but also with potential applications in mind. It is a two-dimensional material, composed of layers of carbon atoms forming six-membered rings. Graphene is the mother of all graphitic forms including zero-dimensional fullerenes, one-dimensional carbon nanotubes and three-dimensional graphite (Fig. 1).[1] Although carbon nanotubes are formed through the rolling of graphene sheets, the properties of the two are quite different. Thus, the electronic and Raman spectra of carbon nanotubes and graphene differ significantly, as do other properties such as electrical conductivity and mechanical strength. A remarkable feature of graphene is that the energy of the electrons is linearly dependent on the wave vector near the crossing points in the Brillouin zone. The charge carriers mimic relativistic particles which can be best described on the basis of the Dirac equation rather than the Schrödinger equation.[1–3] It exhibits fascinating properties such as a room-temperature fractional quantum Hall effect,[2] an ambipolar electric field effect, along with ballistic conduction of charge carriers.[3] Although graphene is supposed to be flat, ripples occur to eliminate the effect of thermal fluctuations.[1] Graphene, as defined, is a single-layer two-dimensional material, but graphene samples with two layers (bi-layer graphene) and more than two but less than ten layers (few-layer graphene) are equally of interest. Most of the physical studies of graphene have been carried out on single-layer sheets obtained by micro-mechanical cleavage techniques,

[a]Chemistry and Physics of Materials Unit, New Chemistry Unit, DST Unit on Nanoscience and CSIR Centre of Excellence in Chemistry, Jawaharlal Nehru Centre for Advanced Scientific Research, Jakkur P. O., Bangalore, 560064, India. E-mail: cnrrao@jncasr.ac.in; Fax: +91 80 22082760
[b]Solid State and Structural Chemistry Unit, Indian Institute of Science, Bangalore, 560012, India

† This paper is part of a Journal of Materials Chemistry theme issue on Layered Materials. Guest editors: Leonardo Marchese and Heloise O. Pastore.

C. N. R. Rao

C. N. R. Rao obtained his PhD from Purdue University and DSc from the University of Mysore. He is a Professor at the Jawaharlal Nehru Centre for Advanced Scientific Research and Honorary Professor at the Indian Institute of Science, and has authored nearly 1200 research papers. He is a member of the Royal Society and the US National Academy of Sciences, and the recipient of the Einstein Gold Medal of UNESCO, Hughes Medal of the Royal Society, the Somiya Award of the International Union of Materials Research Societies, the Dan David Prize for materials research from Israel and the first India Science Prize.

Kanishka Biswas

Kanishka Biswas received his BSc degree from Jadavpur University, Kolkata in 2003. He is a student of the integrated PhD programme (chemical sciences) of Indian Institute of Science, Bangalore and received his MSc (Chemistry) degree in 2006. He has worked primarily on the synthesis, growth and characterization of various inorganic nanomaterials.

View Article Online

Published on 20 January 2009. Downloaded by IIT Jodhpur on 11/2/2023 9:13:43 PM.

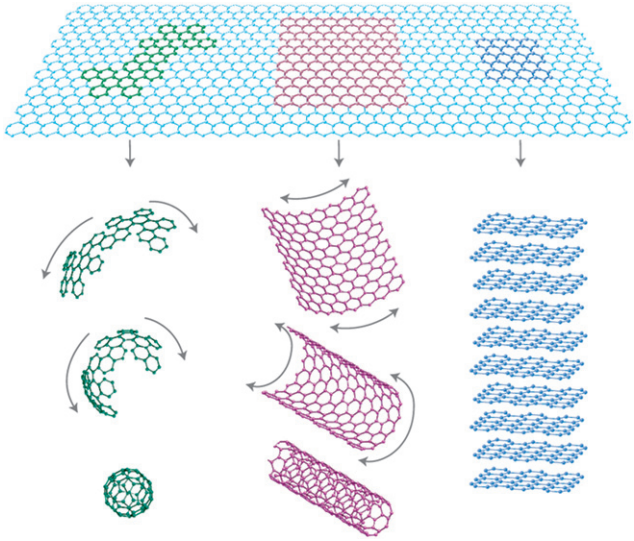

Fig. 1 Graphene: mother of all graphitic forms. (Reproduced with permission from ref. 1).

but the preparation of large quantities of different types of graphene and their characterization is receiving attention recently.[4] In this article, we highlight the synthesis, structure, and properties of different types of graphene. Chemical manipulation of graphene and its surface properties are also described. The extraordinary sensitivity of graphene to electrochemical doping and to molecular charge transfer are examined in some detail.

Single- and bi-layer graphenes

Preparation and characterization

Single and bi-layer graphenes are obtained by micromechanical cleavage of bulk graphite or highly oriented pyrolitic graphite (HOPG), the same technique that allowed the isolation of graphene for the first time by Geim and co-wokers.[3,5] Recently, single- and bi-layer graphenes have been obtained in the gas phase by using a substrate-free, atmospheric-pressure microwave plasma reactor.[6] Thermal decomposition (vacuum graphitization) of SiC has also been employed to obtain epitaxial single- and bi-layer graphenes.[7,8] Single- and bi-layer graphene nanoribbons (width < 10 nm) can be obtained by thermal exfoliation followed by solubilization and centrifugation of expandable graphite.[9] Single-layer graphene is reported to be formed by sonication in water following the chemical reduction of graphitic oxide with hydrazine.[10]

Graphene has been characterized by employing microscopic and spectroscopic techniques.[1] Atomic force microscopy (AFM) is a basic characterization tool-which provides information of the number of graphene layers present in a sample (Fig. 2 a).[5] By differential height measurements at the folded edge, it is possible to obtain the layer thickness. In Fig. 2 a, the differential height is about 4 Å, which is close to the thickness of a monolayer (3.4 Å). Transmission electron microscopy (TEM) provides information on the morphology and the number of layers (see Fig. 2 b).[11] A folded graphene sheet is locally parallel to the electron beam. For single-layer graphene, a fold exhibits one dark line (left panel in Fig. 2 b), similar to the TEM images from one-half of a single-walled carbon nanotube. The right panel in Fig. 2 b shows a folded edge of bi-layer graphene, which exhibits two dark lines, similar to double-walled nanotubes. Direct imaging of lattice atoms and topological defects in single-layer graphene have been accomplished by TEM by using aberration correction in combination with a monochromator.[12] Fig. 2 c shows a high-resolution scanning tunnelling microscope (STM) image of single-layer graphene over a 1 nm^2 area.[13] In the regions identified as consisting of single-layer graphene, a honeycomb structure is observed. Searching for single- or bi-layer graphenes amongst millions of thicker flakes obtained by micromechanical cleavage of HOPG is a difficult task.

Single-layer graphene becomes visible in an optical microscope if placed on top of a Si wafer with a 300 nm thick layer of SiO_2.[5,14,15] Fig. 2 d and e show optical microscope images of graphene on 300 nm SiO_2, imaged with white and green lights respectively. The trace in Fig. 2 e shows step-like changes in the contrast for single-, bi- and tri-layer graphenes. Only

K. S. Subrahmanyam

K. S. Subrahmanyam received his MSc (Chemistry) degree from University of Hyderabad, Hyderabad in 2006. He is a student of PhD programme at the Jawaharlal Nehru Centre for Advanced Scientific Research, Bangalore and received his MSc (Eng.) degree in 2008. He is working on synthesis and characterization of graphenes.

A. Govindaraj

A. Govindaraj obtained his PhD degree from the University of Mysore and is a Senior Scientific Officer at the Indian Institute of Science, and Honorary Faculty Fellow at the Jawaharlal Nehru Centre for Advanced Scientific Research. He works on different types of nanomaterials. He has authored more than 100 research papers and co-authored a book on nanotubes and nanowires.

This journal is © The Royal Society of Chemistry 2009

View Article Online

Published on 20 January 2009. Downloaded by IIT Jodhpur on 11/2/2023 9:13:43 PM.

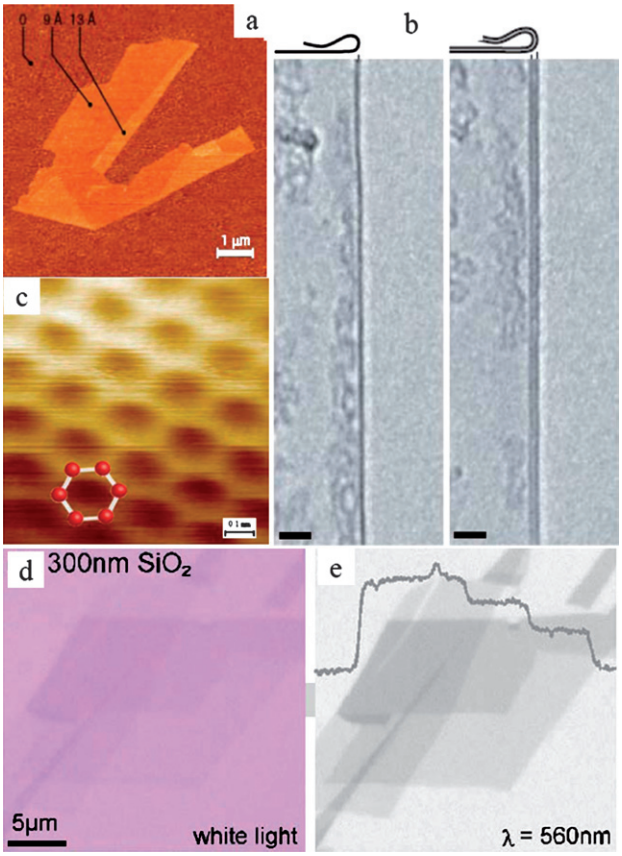

Fig. 2 (a) AFM image of single-layer graphene. The folded edge exhibiting a relative height of ≈4 Å clearly indicates that it is a single-layer graphene. (b) TEM images of folded edges of single-layer and bi-layer graphenes. (c) High-resolution STM images of single-layer graphene. Optical microscope images of graphene crystallites on 300 nm SiO_2 imaged with (d) white light and (e) green light. The trace in (e) shows-step like changes in the contrast for single-, bi- and tri-layer graphenes. (Reproduced with permission from ref. 5, 11, 13 and 14).

a 5% difference in the SiO_2 thickness can make graphene completely invisible.

Raman spectroscopy has proved to be an essential tool to characterize graphene.[16–18] In Fig. 3, we show the Raman spectra of graphenes with increasing the number of layers ($n = 1$ to 19) along with HOPG ($n =$ infinity).[16a] The strongest first order band at 1582 cm^{-1} is the G-band. The intensity of the G-band increases with the increasing numbers of layers. A shoulder around 1600 cm^{-1} on the G-band, designated as the G′ band, appears in few-layer graphenes and this band is defect-related. Another first-order band called the D-band (~1350 cm^{-1}) is inactive in single-layer graphene and is observed generally at the sample edges.[16,17] The D band, which is defect-related, appears as a strong band when the number of graphene layers in a sample is large. The strongest second-order band is observed around 2700 cm^{-1} (2D band).[16–18] Single-layer graphene can be distinguished from bi- and few-layer graphene by the width of the 2D band. The single 2D peak in single-layer graphene often splits into different peaks in bi- and few-layer graphenes. Raman spectra of graphenes are understood on the basis of the double-resonant Raman process involving phonons within the first Brillouin zone of graphite.[16b,16c,18] It is to be noted that though the 2D band is formally the overtone of the D band, the phonon-process and the phonon-electron interaction associated with them are different. The ratio of the intensities of the G and D bands, I_G/I_D is related to the in-plane crystallite size of few-layer graphene samples.[17] The ratio of intensities of the 2D and G bands is sensitive to hole or electron doping, as will be shown later. Changes in the Raman spectra due to changes in the number of layers or due to doping reflect the evolution of the electronic structure and electron–phonon interactions. Temperature-dependent Raman studies on single and bi-layer by Calizo *et al.*[19] have enabled the determination of the temperature coefficient of the G band. It must be noted that the D and 2D bands cannot be used to determine the number of layers, but are useful to investigate electronic effects.

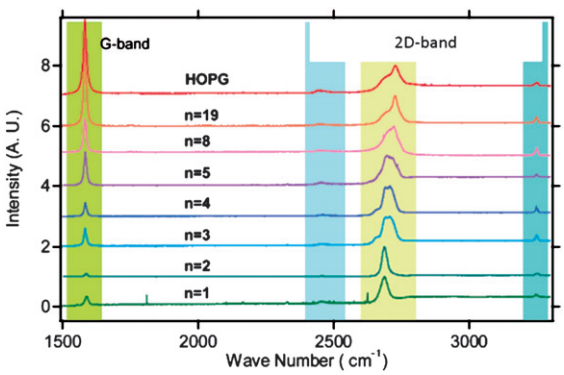

Fig. 3 Raman spectra of graphenes with increasing the number of layers ($n = 1$ to 19) along with HOPG ($n =$ infinity). (Reproduced with permission from ref. 16a).

Structure

Single-layer graphene appears to be a strictly two-dimensional material with a layer of carbon atoms densely packed in a honeycomb crystal lattice. Perfect two-dimensional crystals are thermodynamically unstable and cannot exist.[20–23] The divergent contribution of thermal fluctuations destroys the long-range order, resulting in the melting of the two-dimensional lattice at finite temperatures. TEM and electron diffraction investigations reveal that a suspended single-layer graphene is not perfectly flat, but exhibits intrinsic microscopic roughening such

View Article Online

Published on 20 January 2009. Downloaded by IIT Jodhpur on 11/2/2023 9:13:43 PM.

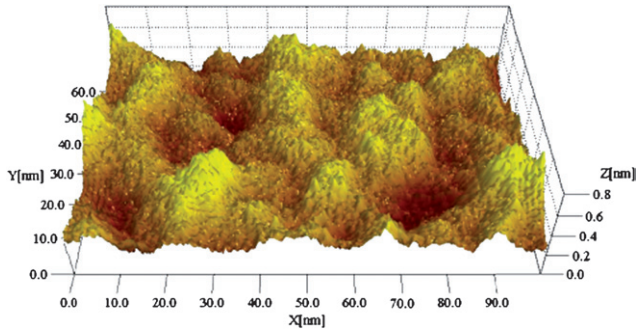

Fig. 4 Stereographic plot of a large-scale (100 × 62 nm) STM image of a single-layer graphene film on the silicon dioxide surface. The STM scanning conditions were $V_{bias} = 1$ V (sample potential) and $I = 0.6$ nA. The 0.8 nm scale of the vertical (Z) coordinate is greatly enlarged to accentuate the surface features. (Reproduced with permission from ref. 13).

that the normal surface varies from its mean direction by several degrees.[11] STM investigations reveal nanometre-scale ripples in single-layer graphene (Fig. 4).[13] The observed height variation is ~0.5 nm, occurring on a lateral scale of ~10 nm. Such gentle crumpling in the third dimension observed on a lateral scale of ~10 nm leads to a gain in elastic energy but suppresses thermal vibrations and minimizes the total free energy above a certain temperature.

Electronic structure and unique properties

Single-layer graphene has two atoms per unit cell, giving rise to two conical points, K and K', per Brillouin zone where band-crossing occurs (Fig. 5). Near these crossing points, the electron energy, E, is linearly dependent on the wave vector. As mentioned earlier, the charge carriers in single-layer graphene mimic relativistic particles and are described using the Dirac equation.[24–28] Although there is nothing relativistic about the electrons moving around the carbon atoms, their interaction with the periodic potential of the honeycomb lattice of graphene gives rise to quasiparticles which are accurately described by the (2 + 1)-dimensional Dirac equation at low E, with an effective speed of light, $v_F \approx 10^6$ m s^{-1}.[1] The quasiparticles, called massless Dirac fermions, are electrons which have lost their rest mass m_0 (or can be considered as neutrinos that have acquired the electron charge e). The Dirac equation is a direct consequence of the crystal symmetry of single-layer graphene. Besides the linear dispersion of E with respect to the wave vector, the electron states of graphene near zero E (where the bands intersect) are composed of states belonging to different sublattices, whose relative contributions in the make-up of quasiparticles has to be taken into account. Because of the linear spectrum, quasiparticles in single-layer graphene are expected to behave differently from those in conventional metals or semiconductors, which exhibit a parabolic free electron-like dispersion relation.

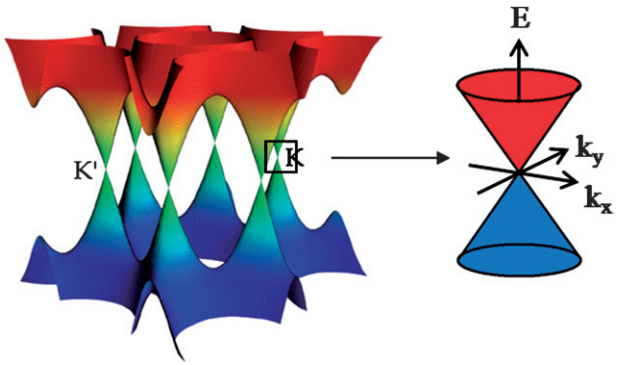

Fig. 5 Electronic band structure of single-layer graphene.

Single-layer graphene exhibits a strong ambipolar electric field effect such that charge carriers can be tuned continuously between electrons and holes in concentrations up to 10^{13} cm^{-2} and room-temperature mobilities of ~10,000 cm^2/V s can be induced by applying gate voltage.[3] Novoselov *et al.*[29] observed a half-integer quantum Hall effect (QHE) at low temperatures, where it shows an uninterrupted ladder of equidistant steps in Hall conductivity which persists through the neutrality (Dirac) point in single-layer graphene (Fig. 6). The sequence is shifted with respect to the standard QHE sequence by a factor of ½. The conductivity of graphene does not fall below a minimum value corresponding to a quantum unit of conductance even when the carrier concentration tends to zero.[29] A room-temperature half-integer QHE has also been observed in single-layer graphene.[2] An electrochemical resonator based on single-layer graphene has been fabricated by Bunch *et al.*[30] Micrometre-size sensors made from single-layer graphene are capable of detecting individual events when gas molecules such as NH_3, CO, H_2O and NO_2 attach to or detach from the surface.[31] The adsorbed molecules change the local carrier concentration leading to step-like changes in resistance.

In the case of bi-layer graphene with two carbon layers, the nearest-neighbour tight-binding approximation predicts a gapless sate with parabolic bands touching at K and K' points, instead of conical bands.[32] Detailed considerations yield a small band overlap at larger energies. Bi-layer graphene can be treated as a gapless semiconductor.[33] The charge carriers have finite mass (massive Dirac fermions). Bi-layer graphene exhibits an equally anomalous QHE.[34] The standard sequence of Hall plateaux has been observed, but the very first plateau at zero carrier concentration was missing (see inset of Fig. 6). This implies that bi-layer graphene remains metallic at the neutrality point.[34] A standard QHE with all the plateaux present can be recovered in bi-layer graphene by applying an electric field. The gate voltage changes the carrier concentration and induces an asymmetry between the two graphene layers, resulting in a semiconducting gap.[35,36]

 This journal is © The Royal Society of Chemistry 2009

View Article Online

Published on 20 January 2009. Downloaded by IIT Jodhpur on 11/2/2023 9:13:43 PM.

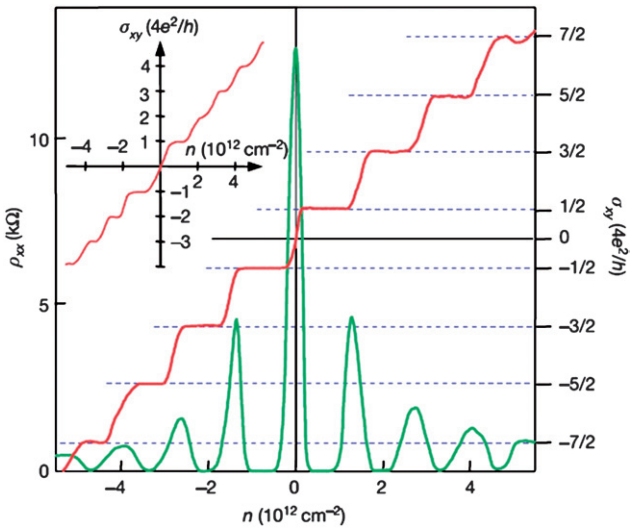

Fig. 6 Hall conductivity (σ_{xy}) and longitudinal resistivity (ρ_{xx}) of single-layer graphene as a function of carrier concentration at $B = 14$ T and $T = 4$K. Inset shows the Hall conductivity of bi-layer graphene. (Reproduced with permission from ref. 29).

Few-layer graphenes

Synthesis and characterization

Micro-mechanical cleavage of HOPG cannot be used for preparing large quantities of graphene required for various investigations and applications. It, therefore, becomes necessary to find methods which can provide graphene in good yields. Several methods have been explored to prepare graphene in large quantities and they generally produce few-layer graphenes. The methods are chemical vapor deposition of camphor (CG),[4,37] conversion of nanodiamond (DG),[4,38] and exfoliation of graphitic oxide (EG).[4,39] In the first method, camphor is pyrolysed over nickel nanoparticles at 770 °C in the presence of argon. The method to prepare DG involves annealing nanodiamond at 1650 °C or higher in an He atmosphere. In the product there is always some diamond-like particles admixed with graphene. The most popular method to prepare graphene is by the exfoliation of graphitic oxide. Graphitic oxide is prepared by reacting graphite with a mixture of concentrated nitric acid and concentrated sulfuric acid with potassium chlorate at room temperature for 5 days.[40] Exfoliation is carried out by giving a sudden thermal shock to graphitic oxide in a long quartz tube at 1050 °C under an Ar atmosphere. It has been recently found that arc evaporation of graphite in the presence of H_2 and He mixtures produces graphene (HG). This method makes use of the fact that the formation of carbon nanotubes is not favored in the presence of H_2 leaving behind the graphene sheets.

Of these different methods, exfoliation of graphite oxide is most commonly used. Graphene samples prepared by different chemical methods have been characterized by various physical methods.

Typical XRD patterns of different graphene samples are shown in Fig. 7 a. The samples show the (002) reflection around 25° as well as the (100) and (101) reflections, merged to give a broad peak around 45°. The sharp graphitic reflection in the powder XRD pattern of CG shows that it comprises a large number of layers. EG and HG show broad peaks in the XRD patterns, while the XRD pattern of DG has reflections corresponding to both small and large graphitic particles. The number of layers in different graphene samples can be obtained by Lorentzian fitting of the (002) reflection making the use of the Scherrer formula. In Fig. 7 b and c, we show multiple Lorentzian fitting of the (002) reflections of the EG and HG samples respectively. In Table 1, we list the number of layers obtained by fitting the (002) reflections. The in-plane crystallite size of graphenes obtained from the (100) reflections are also listed in

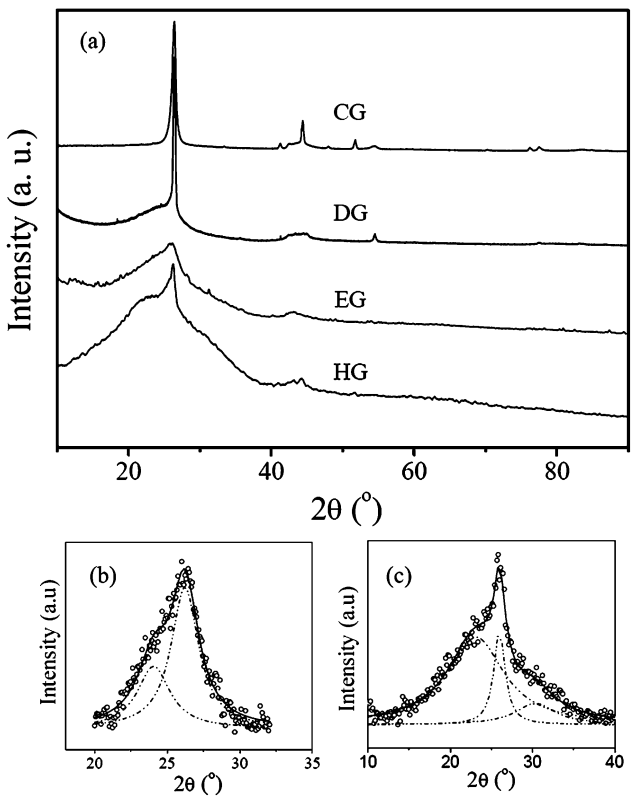

Fig. 7 (a) XRD patterns of CG, DG, EG and HG samples. Multiple Lorentzian fitting of the (002) reflections of (b) EG and (c) HG samples.

View Article Online

Published on 20 January 2009. Downloaded by IIT Jodhpur on 11/2/2023 9:13:43 PM.

Table 1 Number of layers and crystallite sizes from XRD patterns of graphene samples

Graphene Sample	Minimum number of layers from the (002) reflection	In-plane crystallite size from (100) reflection/nm
CG	50	6
DG	6	5
EG	3	5
HG	2	6

the Table 1. The (100) reflection generally overlaps the (101) reflection and has to be deconvoluted to obtain the position and width.

AFM is employed to obtain the number of layers in few-layer graphenes. We show typical AFM images of graphene samples in Fig. 8. AFM cross-section height profile analysis indicates that the CG sample consists of more than 20 layers while EG and DG possess three to six graphene layers. HG has the smallest number of layers.

TEM is used to examine the morphology of few-layer graphenes. TEM images of a few samples are shown in Fig. 9. Large crystalline sheets are observed in the case of CG, while disordered graphene sheets are seen in EG, as can be seen from the images in Fig. 9 a and b, respectively. Small particles with diameters in the 3–20 nm range along with onion-like nanoparticles are found in the TEM image of DG in Fig. 9 c. The TEM image of HG in Fig. 9 d shows few-layer graphene, and the inset in the figure corresponds to the signature of bi-layer graphene.

In Fig. 10, we show Raman spectra of CG, DG, EG and HG graphenes and the band positions are presented in Table 2. We see intense D and G′ bands both of which are defect related. The in-plane crystallite sizes (L_a) are calculated from the Raman spectra of the graphene samples by employing the relation $L_a = 4.4\ (I_G/I_D)$.[17] The G band position varies from sample to sample because of the difference in the number of layers.

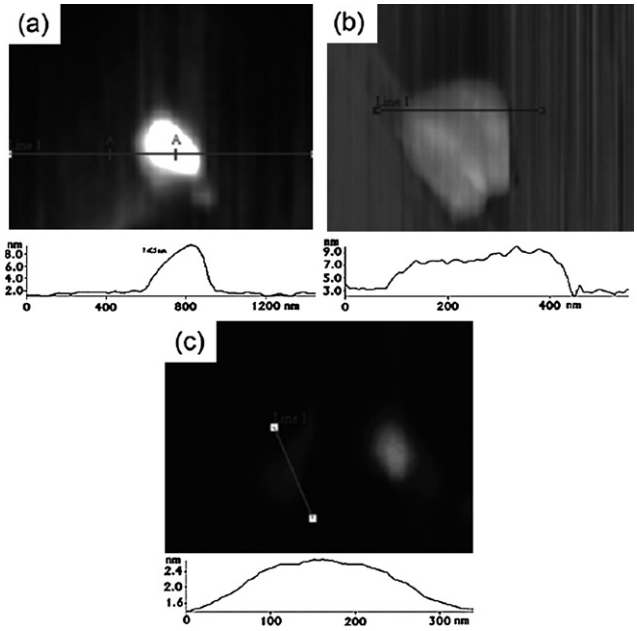

Fig. 8 AFM images and height profiles of graphene samples: (a) CG, (b) EG and (c) DG. (Reproduced with permission from ref. 4a).

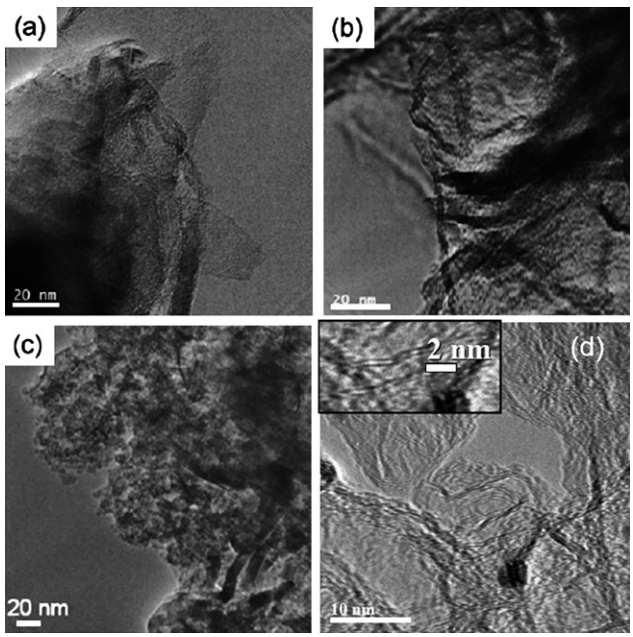

Fig. 9 TEM images of (a) CG, (b) EG, (c) DG and (d) HG samples. Inset in (d) shows the bi-layer feature of HG. ((a), (b) and (c) reproduced with permission from ref. 4a).

Surface and gas adsorption properties

Surface areas of different graphene samples have been measured by the Brunauer–Emmett–Teller (BET) method (Table 3). In Fig. 11 a, we show the typical nitrogen adsorption and desorption curves of a few-layer EG sample. Single-layer graphene is predicted to have a large surface area close to 2600 m^2/g.[41] Few-layer graphenes show large surface areas, some of them approaching the value of single layer graphene.

Hydrogen uptakes of different graphene samples have been investigated.[42] In Fig. 11 b H_2 adsorption and desorption curves of the EG sample are shown. Hysteresis occurs due to the weak interaction between the H_2 and the graphene, and due to pore heterogeneity. H_2 adsorption measurements at 1 atm and 77

 This journal is © The Royal Society of Chemistry 2009

View Article Online

Published on 20 January 2009. Downloaded by IIT Jodhpur on 11/2/2023 9:13:43 PM.

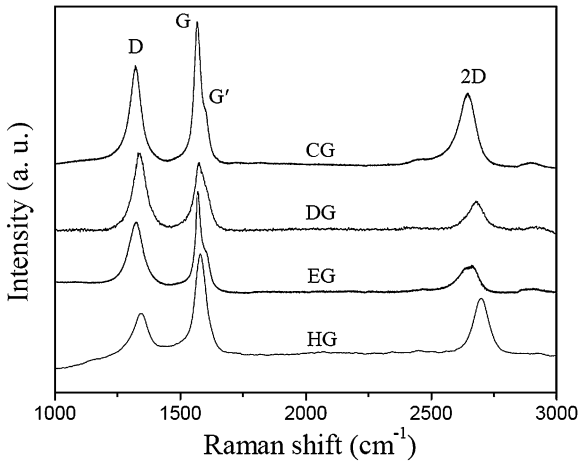

Fig. 10 Raman spectra of (a) CG, (b) DG (c) EG and (d) HG.

Table 2 Raman bands (cm^{-1}) and in-plane crystallite sizes for few-layer graphenes

Graphene sample	D	G	G′	2D	G + D	I_G/I_D	In-plane crystallite size/nm
CG	1321	1567	1604	2647	2919	2.4	10
DG	1332	1576	1606	2678	2909	0.8	4
EG	1324	1569	1605	2652	2908	1.4	6
HG	1329	1560	1597	2665	2920	1.6	7

Table 3 Surface areas and H_2 and CO_2 uptake values of few-layer graphenes

Graphene sample	Surface area (m^2/g) at (1 atm, 77 K)	H_2 uptake (% wt) at (1 atm, 77 K)	High pressure H_2 uptake (% wt) at (100 bar, 300 K)	CO_2 uptake (% wt) at (1 atm, 195 K)
EG	1550	1.7	3.1	34
DG	1013	1.21	2.5	32
HG	680	1	2	17

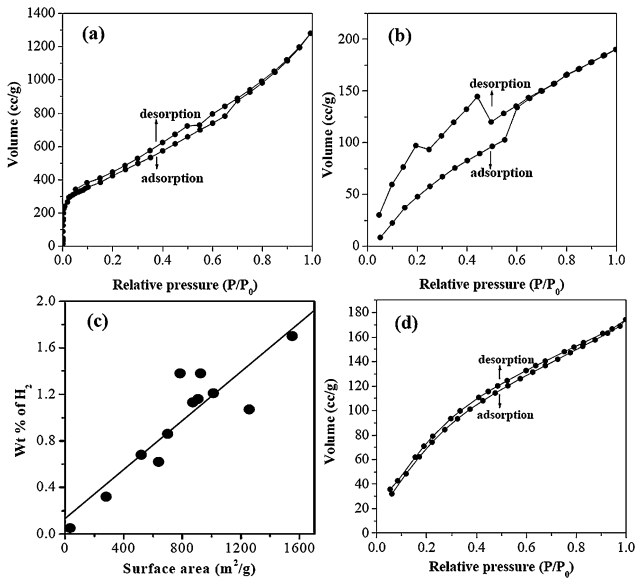

Fig. 11 (a) N_2 and (b) H_2 adsorption isotherms of EG at 1 atm and 77 K; (c) linear relationship between the BET surface area and wt% of H_2 uptake at 1 atm and 77 K and (d) CO_2 adsorption isotherms of EG at 1 atm and 195 K. (Reproduced with permission from ref. 42).

K show that DG, EG and HG can absorb 1.2, 1.7 and 1.0 wt% of H_2 (Table 3). These samples show higher uptakes at 100 bar and 300 K, the values being 2.5, 3.1 and 2.0 wt% for DG, EG and HG, respectively. The values of the H_2 uptake at 1 atm and 77 K by the various graphene samples vary linearly with the surface area as shown by Fig. 11 c. By extrapolation of this plot to the surface area of single-layer graphene, we estimate its H_2 uptake to be around 3 wt% at 1 atm and 77 K. This is impressive. Though the H_2 uptakes of the graphenes described here are low compared to the 6.0 wt% target of the US Department of Energy,[43] there is scope for significant improvement, by producing samples with a smaller number of layers and higher surface areas. It is possible that single layer graphene will exhibit 5–6 wt% of H_2 uptake at 100 atm and 300 K. First-principles calculations show that the H_2 molecule sits alternatively in parallel and perpendicular orientations on the six-membered rings of graphene layer and that single-layer graphene can accommodate up to 7.7 wt% of hydrogen.[42]

CO_2 uptake of few-layer graphenes at 1 atm and 195 K is considerable as shown in Table 3. Fig. 11 d shows typical CO_2 adsorption and desorption curves of the EG sample. First-principles calculations show that CO_2 molecules sit alternatively in a parallel fashion on the six-membered rings to giving use to a maximum uptake of 37.9 wt% in the case of single-layer graphene.[42]

Functionalization and solubilization

Single-walled carbon nanotubes (SWNTs) have been functionalized by both covalent and non-covalent means in order to solubilize them in different solvents.[44,45] Few-layer graphene has also been functionalized using different methods through covalent and non-covalent modifications. One of the simple methods is the derivatization of graphene with a long-chain alkyl amide, accomplished by acid treatment followed by reaction with thionylchloride and dodecylamine.[4,46] Amide-functionalized graphene is soluble in organic solvents such as tetrahydrofuran (THF), carbon tetrachloride (CCl_4) and dichloromethane (DCM), as shown in the photograph in Fig. 12 a. The reaction of graphene with a mixture of

View Article Online

Published on 20 January 2009. Downloaded by IIT Jodhpur on 11/2/2023 9:13:43 PM.

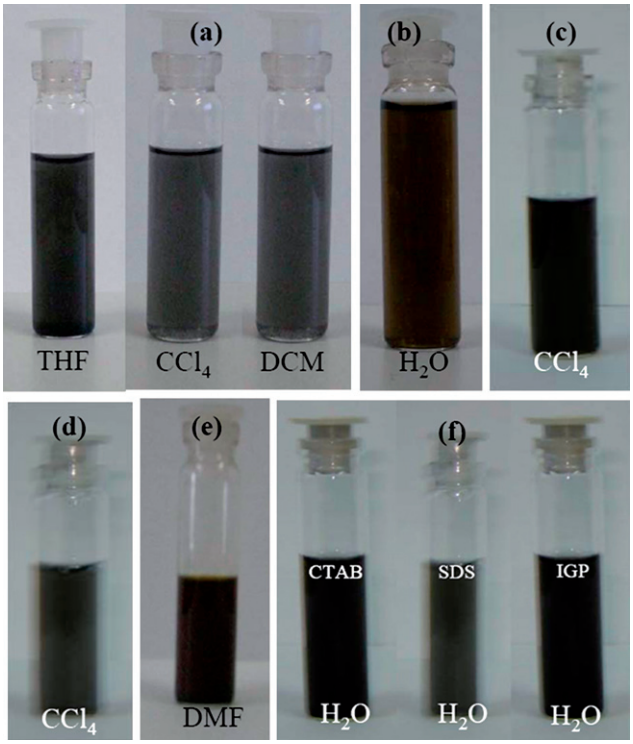

Fig. 12 Photographs of (a) dispersions of the amide-functionalized EG in THF, CCl_4 and dichloromethane, (b) water soluble EG, (c) dispersion of HDTMS treated EG in CCl_4, (d) dispersion of DBDT treated EG in CCl_4, (e) dispersion of PYBS treated EG in DMF and (f) water dispersions of EG treated with CTAB, SDS and IGP. ((a) and (b) reproduced with permission from ref. 4a).

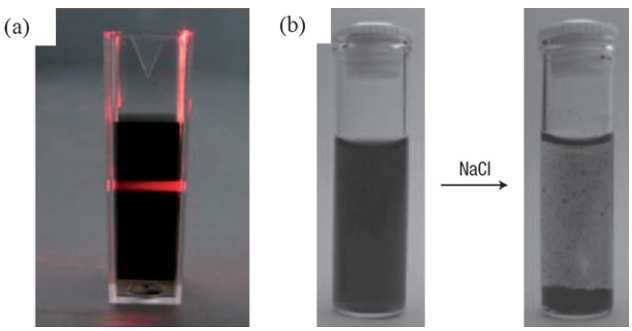

Fig. 13 (a) Tyndall effect and (b) Salt effect confirming the colloidal nature of graphene dispersed in water by electrostatic stabilization. (Reproduced with permission from ref. 48).

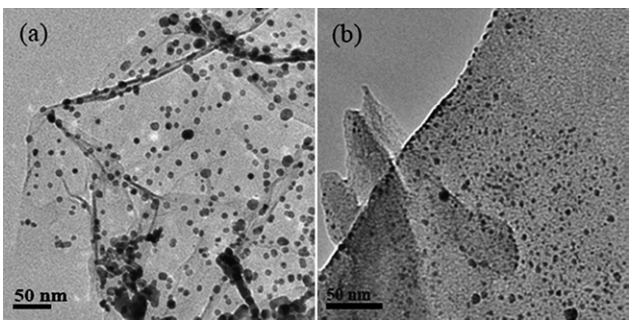

Fig. 14 TEM images of decorated EG with (a) Pt and (b) Ag nanoparticles.

concentrated H_2SO_4 and HNO_3 gives water-soluble graphene which is stable for several months (photograph in Fig. 12 b). Graphene can also be made soluble in H_2O by sulfonation[47] and electrostatic stabilization.[48] Graphene is solubilized in CCl_4 by interaction with organosilane and organotin reagents such as hexadecyltrimethoxysilane (HDTMS) (photograph in Fig. 12 c) and dibutyldimethoxytin (DBDT) (photograph in Fig. 12 d).[49]

Graphene can be functionalized through non-covalent modification without affecting its electronic structure by employing different methods such as wrapping with polyethylene glycol (PEG) and other surfactants, or π–π interaction with a pyrene derivative such as 1-pyrenebutanoicacid succinimidyl ester (PYBS).[4,49] Wrapping with PEG gives water-soluble graphene. By π–π interaction with PYBS, graphene becomes soluble in dimethylformamide, as shown in the photograph in Fig. 12 e. Non-covalent interaction of graphene with surfactants such as Igepal CO-890 (polyoxyethylene (40) nonylphenylether, IGP), sodium dodecylsulfate (SDS) and cetyltrimethylammoniumbromide (CTAB) gives water-soluble graphene. Fig. 12 f shows photographs of water-soluble graphene obtained with IGP, SDS and CTAB. In Fig. 13 a we show the graphene dispersion obtained by the electrostatic stabilization giving rise to a Tyndall effect, in which a laser beam passing through a colloidal solution leaves a discernible track as a result of light scattering.[48] Adding an electrolyte solution into the dispersion leads to immediate coagulation (Fig. 13 b).[48]

Decoration with metal nanoparticles

Carbon nanotubes decorated by metal nanoparticles are expected to be useful in catalysis, nanoelectronics, optics and nanobiotechnology.[44] Graphene can also be decorated by metal nanoparticles.[50] In Fig. 14 a and b, we show TEM images of EG decorated with platinum and silver nanoparticles.[4b] These samples were decorated with the metal nanoparticles in a single step through the polyol reduction method using chloroplatinic acid and silver nitrate. On coating with these metal particles the Raman D band intensity increases while the 2D band intensity

 This journal is © The Royal Society of Chemistry 2009

View Article Online

Published on 20 January 2009. Downloaded by IIT Jodhpur on 11/2/2023 9:13:43 PM.

decreases, showing the effect of Coulombic charge transfer.

Electrochemical properties

Activated carbon, graphite fibers and such carbon structures have been widely used in electrochemical applications. Electrochemical properties of graphenes prepared by different methods have been investigated using the redox reactions with potassium ferrocyanide.[4,51] The behavior of EG is similar to that of the basal plane in graphite while DG and CG exhibit slightly better kinetics. Different graphene samples have been investigated as the electrode materials in electrochemical supercapacitors using aq. H_2SO_4 and an ionic liquid (*N*-butyl-*N*-methylpyrrolidinium bis(trifluoromethanesulfonyl)imide, $PYR_{14}TFSI$) as electrolytes.[4,51] EG and DG exhibit high specific capacitance in aq. H_2SO_4, the value reaching up to 117 and 35 F/g. We show in Fig. 15 a voltammetric characteristics of a capacitor built from graphene electrodes (5 mg each), at a scan rate of 100 mV/s using aqueous H_2SO_4 (1 M). Fig. 15 b shows specific capacitance as a function of scan rate for different graphene samples. By using the ionic liquid, the operating voltage has been extended to 3.5 V (instead of 1 V in the case of aq. H_2SO_4), the specific capacitance values being 75 and 40 F/g for EG and DG respectively.

Magnetic properties

The electronic properties of graphene depend on the nature of the edges.[52–54] For example, the zigzag edges in a graphene sheet have nonbonding-electrons giving rise to edge states. The edge states can cause rather unconventional magnetism including ferromagnetism, spin glass behaviour and magnetic switching phenomena. Thus, mono-hydrogenated and di-hydrogenated zigzag edges give rise to ferromagnetism in graphene. Substitution of hydrogen atoms by fluorine affects the magnetic properties. Graphene prepared by heating nanodiamond particles shows Pauli paramagnetic susceptibility or spin paramagnetic susceptibility of the π-electrons, whose value is one to two orders of magnitude larger than that of bulk graphite. Activated carbon fibers

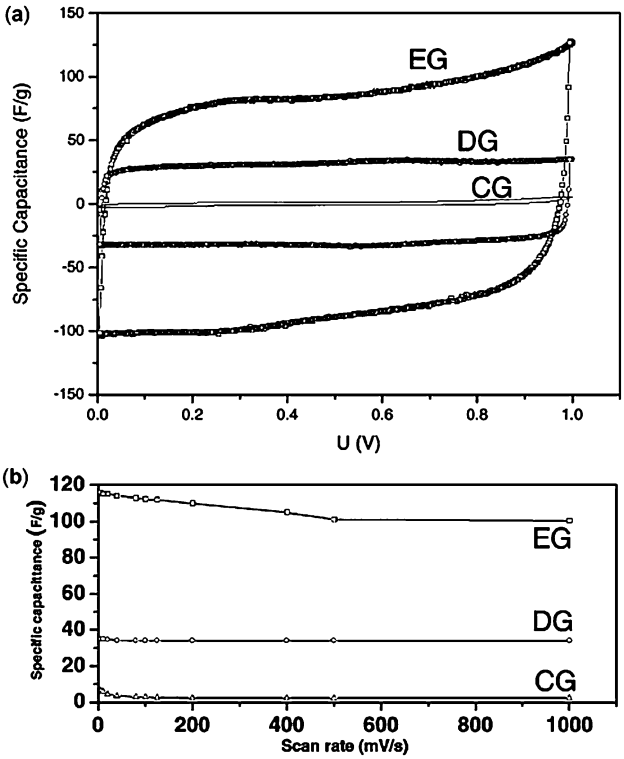

Fig. 15 (a) Voltammetric characteristics of a capacitor built from different graphene electrodes (5 mg each) at a scan rate of 100 mV/s using aqueous H_2SO_4 (1 M) and (b) specific capacitance as a function of scan rate.

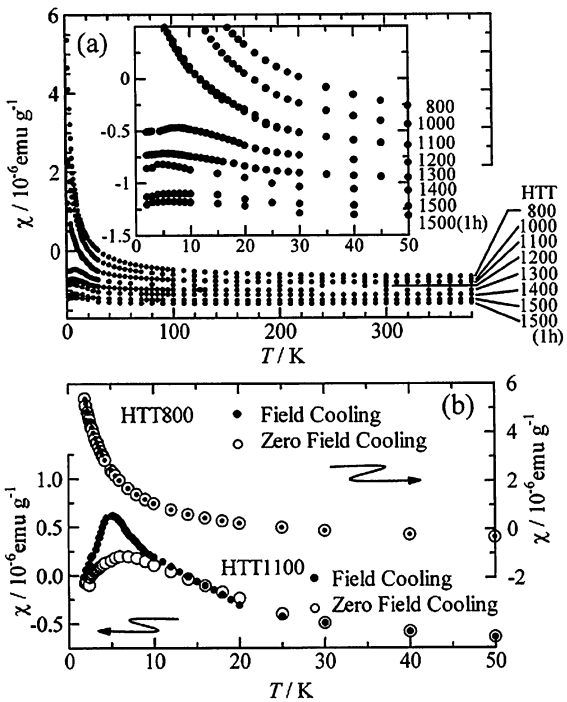

Fig. 16 (a) Magnetic susceptibility (χ) *vs.* temperature plots under $H = 1$ T for the activated carbon fibers heat treated at up to 1500 °C. Inset shows the detailed behaviour. (b) Field cooling effects on χ for samples heated at 800 and 1100 °C respectively, where the open and solid symbols correspond to the data on zero-field and field (1 T) cooling runs, respectively. (Reproduced with permission from ref. 55).

View Article Online

Published on 20 January 2009. Downloaded by IIT Jodhpur on 11/2/2023 9:13:43 PM.

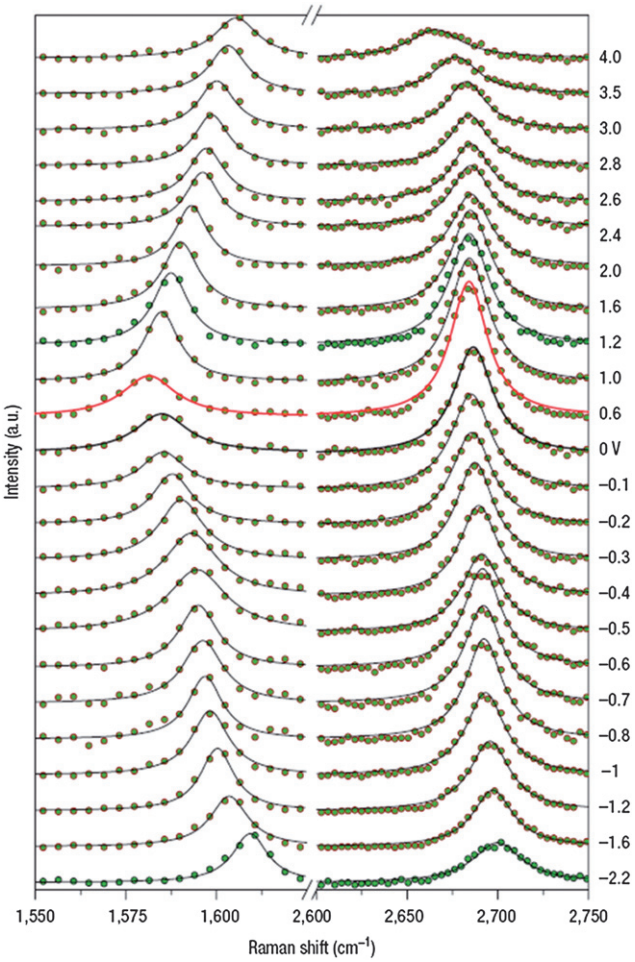

Fig. 17 Raman spectra of graphene as a function of gate voltage (−2.2 to +4.0 V). The dots are the experimental data, the black lines are fitted Lorentzians, and the red line corresponds to the Dirac point. The G band is on the left and the 2D band is on the right. (Reproduced with permission from ref. 57).

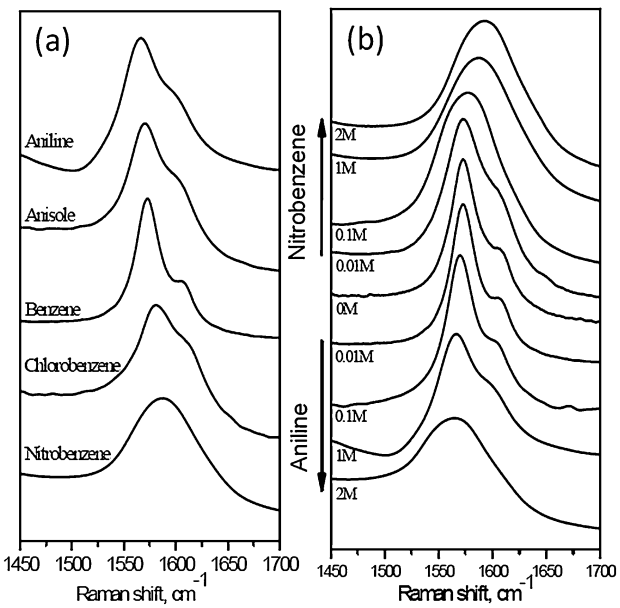

Fig. 18 Raman shift of the G band of graphene on interaction with (a) 1 M solutions of mono-substituted benzenes and (b) with varying concentrations of aniline and nitrobenzene. (Reproduced with permission from ref. 58).

consist of a three-dimensional disordered network of graphene domains, where each domain is featured with stacking of 3–4 layers of graphene and having an in-plane crystallite size of 2–3 nm. The magnetic susceptibility of pristine activated carbon fibers heated to different temperatures shows Cuire–Weiss type behaviour (Fig. 16 a) which indicates the presence of localized magnetic moments at the edges of graphene.[55] The presence of a small cusp at 7 K in Fig. 16 b, and the large field-cooling effect are due to the development of quenched disordered magnetic structures like the spin-glass sate in a sample heated at 1100 °C. Preliminary studies on the magnetic properties of the graphene prepared by other methods also show similar Cuire–Weiss type magnetic features as well as divergence between field-cooled and zero field-cooled samples. They all show magnetic hysteresis at low temperatures. Of the various samples studied, HG shows the highest magnetization and Cuire–Weiss temperature. It would appear that one can tailor the magnetism by cutting graphene sheets in different directions or by chemical modification.

Physical adsorption of molecules on graphene causes changes in the electronic states and the magnetic properties, depending on the nature of the molecules.[52,53] The edge-state spins of graphene can be employed to detect the helium in nanopores. Physical adsorption of oxygen results in a large magnetoresistance of the nanographene network.[54] On the other hand, confinement of potassium clusters in the nanopores surrounded by nanographene domain yields a nonmagnetic domain.[54]

Binding of DNA nucleobases and nucleosides

Interaction of graphene with DNA nucleobases and nucleosides has been investigated by isothermal titration calorimetry.[56] The order of interaction energies of the nucleobases varies as guanine (G) > adenine (A) > cytosine (C) > thymine (T) in aqueous solution, although the positions of C and T seem to be interchangeable. The same trend is found with the nucleosides. Interaction energies of A–T and G–C pairs are somewhere between those of the constituent bases. Theoretical calculations including van der Waals interaction and

 This journal is © The Royal Society of Chemistry 2009

View Article Online

Published on 20 January 2009. Downloaded by IIT Jodhpur on 11/2/2023 9:13:43 PM.

solvation energy give the trend to be G > A ~ T > C.

Changes in the electronic structure and properties induced by doping and molecular charge-transfer

It has been demonstrated recently that a top-gated single-layer graphene transistor is able to reach doping levels up to 5 $\times$ 10^{13} cm^{-2} by employing *in-situ* Raman measurements to monitor doping.[57] The G band stiffens and sharpens for both electron- and hole-doping, but the 2D band shows a different response to holes and electrons (Fig. 17). The ratio of the intensities of the G and 2D bands shows a strong dependence on doping, making it a sensitive parameter to monitor doping.

Electron-donor and -acceptor molecules also have marked effects on the electronic structure and properties of graphene.[58,59] Thus, electron-donor molecules, such as aniline and tetrathiafulvalene (TTF), soften the Raman G band while electron-acceptor molecules, such as nitrobenzene and tetracyanoethylene (TCNE), stiffen the G band. In Fig 18 a, we show typical G bands of a few-layer graphene after interaction with 1 M solutions of various mono-substituted benzenes with electron-donating and -withdrawing groups. The magnitude of softening and stiffening of the G band can be tuned by changing the concentrations of the electron-donating and -withdrawing molecules, as shown in Fig. 18 b. The width of the G band increases on interaction with these molecules. The width of the D band also varies on the interaction with electron-donor and -acceptor molecules. The 2D band intensity decreases markedly on interaction with electron-donor and -acceptor molecules, as can be seen from Fig. 19 a. The ratio of intensities of the 2D and G bands, I_{2D}/I_G, is a sensitive probe to examine the effect of the electron-donor and -acceptor molecules on the electronic structure of graphene. In Fig. 19 b, we show how the I_{2D}/I_G ratio decreases markedly with the concentration of both TTF and TCNE. The I_D/I_G intensity ratio shows an opposite trend. This is because the origins of D and 2D bands are quite different. The electrical conductivity of graphene also varies on interaction with both electron-donor and -acceptor molecules (Fig. 20). Electron-donor molecules decrease the conductivity of graphene while electron-acceptor molecules increase the conductivity. Adsorption of H_2O, NH_3, CO, NO_2 and NO on graphene is also related to the charge-transfer between the molecules and the graphene surface.[60] The magnetic moment of molecules also seems to influence the doping efficiency.

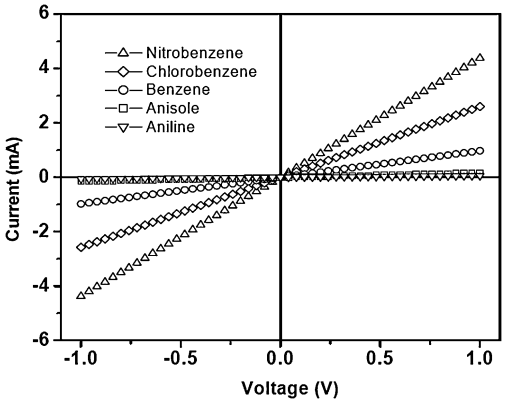

Fig. 20 *I–V* characteristics of the graphene in the presence of benzene and 1 M solutions of nitrobenzene, chlorobenzene, anisole and aniline in benzene. (Reproduced with permission from ref. 58).

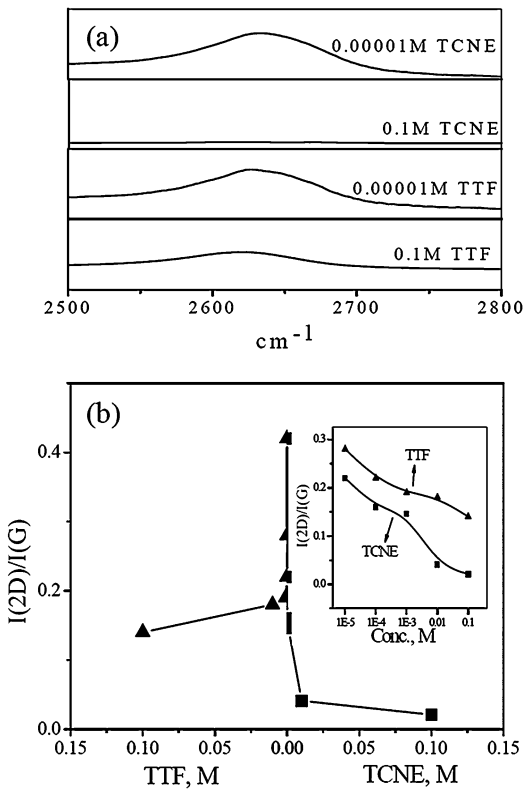

Fig. 19 Variation in the (a) Raman 2D-bands and the (b) 2D/G intensity ratio of graphene with the concentration of TTF and TCNE. Inset in (b) shows the plots of I_{2D}/I_G against logarithm of the concentration. (Reproduced with permission from ref. 59).

Outlook

The above presentation should indicate how research on graphene has become exciting in the last three years, although there are many aspects yet to be investigated. Even the synthesis of graphenes has to be put on firm ground, wherein

View Article Online

Published on 20 January 2009. Downloaded by IIT Jodhpur on 11/2/2023 9:13:43 PM.

reliable procedures become available to prepare samples with the desired number of layers. Many of the properties of graphene are yet to be explored. These include sensor properties of few-layer graphene as well as electrical, magnetic and other properties. For example, it would be of great interest to dope graphene with nitrogen and boron and study the effect on electrical properties. The magnetic properties of graphenes prepared by different methods need to be studied to understand factors responsible for magnetism. The polystyrene-graphene composite has been shown to exhibit a percolation threshold of ~0.1 V% for room temperature electrical conductivity and it shows a conductivity of ~ 0.1 Sm^{-1} at only 1 V%.[61] 1 wt% of functionalized graphene in poly(acrylonitrile) increases the glass transition temperature of the polymer and improves the elastic modulus, strength and thermal stability.[62] The mechanical properties of polyvinyl alcohol and poly(methyl methacrylate) composites reinforced with functionalized few-layer graphene show a significant increase in both the elastic modulus and hardness with the addition of 0.6 wt% of the graphene.[63] The crystallinity of polyvinyl alcohol also increases with the addition of few-layer graphene. Detailed investigations on the electrical and mechanical properties of graphene-based polymer composites are necessary, however. Non-linear optical properties of graphene in solution as well as hydrogen adsorption properties of single- and bi-layer graphene are important problems. Recent results on the effect of molecular charge transfer on few-layer graphene suggest that careful studies need to be carried out with single- and bi-layer graphenes. Transformation of graphenes to nanotubes would also be interesting to examine. In addition to experimental studies, there is considerable scope for theoretical investigations of various aspects of graphene, including electronic structure, doping effects and dependence of properties on the number of layers.

References

1 A. K. Geim and K. S. Novoselov, *Nature Mater.*, 2007, **6**, 183.
2 K. S. Novoselov, Z. Jiang, Y. Zhang, S. V. Morozov, H. L. Stormer, U. Zeitler, J. C. Maan, G. S. Boebinger, P. Kim and A. K. Geim, *Science*, 2007, **315**, 1379.
3 K. S. Novoselov, A. K. Geim, S. V. Morozov, D. Jiang, Y. Zhang, S. V. Dubonos, I. V. Grigorieva and A. A. Firsov, *Science*, 2004, **306**, 666.
4 (*a*) K. S. Subrahmanyam, S. R. C. Vivekchand, A. Govindaraj and C. N. R. Rao, *J. Mater. Chem.*, 2008, **18**, 2007; (*b*) K. S. Subrahmanyam, *MSc (Eng) Thesis*, Jawaharlal Nehru Centre for Advanced Scientific Research, Bangalore, 2008.
5 K. S. Novoselov, D. Jiang, F. Schedin, T. J. Booth, V. V. Khotkevich, S. V. Morozov and A. K. Geim, *Proc. Natl. Acad. Sci. USA*, 2005, **102**, 10451.
6 A. Dato, V. Radmilovic, Z. Lee, J. Phillips and M. Frenklach, *Nano Lett.*, 2008, **8**, 2012.
7 C. Berger, Z. Song, X. Li, X. Wu, N. Brown, C. Naud, D. Mayou, T. Li, J. Hass, A. N. Marchenkov, E. H. Conrad, P. N. First and W. A. de Heer, *Science*, 2004, **312**, 1191.
8 T. Ohta, A. Bostwick, T. Seyller, K. Horn and E. Rotenberg, *Science*, 2004, **313**, 951.
9 X. Li, X. Wang, L. Zhang, S. Lee and H. Dai, *Science*, 2008, **319**, 1229.
10 S. Gilje, S. Han, M. Wang, K. L. Wang and R. B. Kaner, *Nano Lett.*, 2007, **7**, 3394.
11 J. C. Meyer, A. K. Geim, M. I. Katsnelson, K. S. Novoselov, T. J. Booth and S. Roth, *Nature*, 2007, **446**, 60.
12 J. C. Meyer, C. Kisielowski, R. Erni, M. D. Rossell, M. F. Crommie and A. Zettl, *Nano Lett.*, 2008, **8**, 3582.
13 E. Stolyarova, R. K. Taeg, S. Ryu, J. Maultzsch, P. Kim, L. E. Brus, T. F. Heinz, M. S. Hybertsen and G. W. Flynn, *Proc. Natl. Acad. Sci., USA*, 2007, **104**, 9209.
14 P. Blake, E. W. Hill, A. H. C. Neto, K. S. Novoselov, D. Jiang, R. Yang, T. J. Booth and A. K. Geim, *Appl. Phys. Lett.*, 2007, **91**, 63124.
15 S. Roddaro, P. Pingue, V. Piazza, V. Pellegrini and F. Beltram, *Nano Lett.*, 2007, **7**, 2707.
16 (*a*) A. Gupta, G. Chen, P. Joshi, S. Tadigadapa and P. C. Eklund, *Nano Lett.*, 2006, **6**, 2667; (*b*) A. C. Ferrari, *Solidstate Commun.*, 2007, **143**, 47; (*c*) A. C. Ferrari, J. C. Meyer, V. Scardaci, C. Casiraghi, M. Lazzeri, F. Mauri, S. Piscanec, D. Jiang, K. S. Novoselov, S. Roth and A. K. Geim, *Phys. Rev. Lett.*, 2006, **97**, 187401.
17 M. A. Pimenta, G. Dresselhaus, M. S. Dresselhaus, L. A. Cancado, A. Jorio and R. Sato, *Phys. Chem. Chem. Phys.*, 2007, **9**, 1276.
18 D. Graft, F. Molitor, K. Ensslin, C. Stampfer, A. Jungen, C. Hierold and L. Wirtz, *Nano Lett.*, 2007, **7**, 238.
19 I. Calizo, A. A. Balandin, W. Bao, F. Miao and C. N. Lau, *Nano Lett.*, 2007, **7**, 2645.
20 R. E. Peierls, *Ann. I.H. Poincare*, 1935, **5**, 177.
21 L. D. Landau, *Phys. Z. Sowjetunion*, 1937, **11**, 26.
22 L. D. Landau and E. M. Lifshitz, *Statistical Physics, Part I*, Pergamon, Oxford, 1980.
23 N. D. Mermin, *Phys. Rev.*, 1968, **176**, 250.
24 G. W. Semenoff, *Phys. Rev. Lett.*, 1984, **53**, 2449.
25 F. D. M. Haldane, *Phys. Rev. Lett.*, 1988, **61**, 2015.
26 A. M. J. Schakel, *Phys. Rev. D*, 1991, **43**, 1428.
27 J. González, F. Guinea and M. A. H. Vozmediano, *Phys. Rev. Lett.*, 1996, **77**, 3589.
28 M. I. Katsnelson, K. S. Novoselov and A. K. Geim, *Nature Phys.*, 2006, **2**, 620.
29 K. S. Novoselov, A. K. Geim, S. V. Morozov, D. Jiang, M. I. Katsnelson, I. V. Grigorieva, S. V. Dubonos and A. A. Firsov, *Nature*, 2005, **438**, 197.
30 J. S. Bunch, A. M. V. D. Zande, S. S. Verbridge, I. W. Frank, D. M. Tanenbaum, J. M. Parpia, H. G. Craighead and P. L. McEuen, *Science*, 2007, **315**, 490.
31 F. Schedin, A. K. Geim, S. V. Morozov, E. W. Hill, P. Blake, M. I. Katsnelson and K. S. Novoselov, *Nature Mater.*, 2007, **6**, 652.
32 K. S. Novoselov, E. McCann, S. V. Morozov, V. I. Fal'ko, M. I. Katsnelson, U. Zeitler, D. Jiang, F. Schedin and A. K. Geim, *Nat. Phys.*, 2006, **2**, 177.
33 B. Partoens and F. M. Peeters, *Phys. Rev. B*, 2006, **74**, 075404.
34 K. S. Novoselov, E. McCann, S. V. Morozov, V. I. Fal'ko, M. I. Katsnelson, U. Zeitler, D. Jiang, F. Schedin and A. K. Geim, *Nature Nanotechnol.*, 2006, **2**, 177.
35 E. McCann, *Phys. Rev. B*, 2006, **74**, 161403.
36 E. V. Castro, K. S. Novoselov, S. V. Morozov, N. M. R. Peres, J. M. B. Lopes dos Santos, J. Nilsson, F. Guinea, A. K. Geim and A. H. Castro Neto, *Phys. Rev. Lett.*, 2007, **99**, 216802.
37 P. R. Somani, S. P. Somani and M. Umeno, *Chem. Phys. Lett.*, 2006, **430**, 56.
38 O. E. Andersson, B. L. V. Prasad, H. Sato, T. Enoki, Y. Hishiyama, Y. Kaburagi, M. Yoshikawa and S. Bandow, *Phys. Rev. B*, 1998, **58**, 16387.
39 H. C. Schniepp, J.-L. Li, M. J. McAllister, H. Sai, M. Herrera-Alonso, D. H. Adamson, R. K. Prud'homme, R. Car, D. A. Saville and I. A. Aksay, *J. Phys. Chem. B*, 2006, **110**, 8535.
40 L. Staudenmaier, *Ber. Dtsch. Chem. Ges.*, 1898, **31**, 1481.
41 A. Peigney, Ch. Laurent, E. Flahaut, R. R. Bacsa and A. Rousset, *Carbon*, 2001, **39**, 507.
42 A. Ghosh, K. S. Subrahmanyam, K. S. Krishna, S. Datta, A. Govindaraj, S. K. Pati and C. N. R. Rao, *J. Phys. Chem. C*, 2008, **112**, 15704.
43 Multi-Year Research, *Development and Demonstration Plan: Planned Program Activities for 2003–2010: Technical Plan*; US Department of Energy; http://www.eere.energy.gov/hydrogenandfuelcells/mypp/pdfs/storage.pdf.
44 C. N. R. Rao and A. Govindaraj, *Nanotubes and Nanowires, RSC series on Nanoscience*, Royal Society of Chemistry, London, 2006.
45 *Nanomaterials Chemistry: Recent Devolopments*, ed. C. N. R. Rao, A. K. Cheetham and A. Muller, Wiley-VCH, Weinheim, 2007.

 This journal is © The Royal Society of Chemistry 2009

View Article Online

46 S. Niyogi, E. Bekyarova, M. I. Itkis, J. L. McWilliams, M. A. Hamon and R. C. Haddon, *J. Am. Chem. Soc.*, 2006, **128**, 7720.
47 Y. Si and E. T. Samulski, *Nano Lett.*, 2008, **6**, 1679.
48 D. Li, M. B. Muller, S. Gilje, R. B. Kaner and G. Wallace, *Nature Nanotechnol.*, 2008, **3**, 101.
49 K. S. Subrahmanyam, A. Ghosh, A. Gomathi, A. Govindaraj and C. N. R. Rao, *Nanosci. Nanotech. Letts.*, 2008, DOI: 10.1166/nnl.2009.1014.
50 R. Muszynski, B. Seger and P. V. Kamat, *J. Phys. Chem. C*, 2008, **112**, 5263.
51 S. R. C. Vivekchand, C. S. Rout, K. S. Subrahmanyam, A. Govindaraj and C. N. R. Rao, *J. Chem. Sci.*, 2008, **120**, 9.
52 T. Enoki, Y. Kobayashi and K. Fukui, *Int. Rev. Phys. Chem.*, 2008, **26**, 609.
53 T. Enoki and Y. Kobayashi, *J. Mater. Chem.*, 2005, **15**, 3999.
54 T. Enoki and K. Takai, *Dalton Trans.*, 2008, 3773.
55 T. Enoki, N. Kawatsu, Y. Shibayama, H. Sato, R. Kobori, S. Maruyama and K. Kaneko, *Polyhedron*, 2001, **20**, 1311.
56 N. Varghese, U. Mogera, A. Govindaraj, A. Das, P. K. Maiti, A. K. Sood and C. N. R. Rao, *Chem. Phys. Chem.*, 2008, **10**, 206.
57 A. Das, S. Pisana, B. Chakraborty, S. Piscanec, S. K. Saha, U. V. Waghmare, K. S. Novoselov, H. R. Krishnamurthy, A. K. Geim, A. C. Ferrari and A. K. Sood, *Nature Nanotechnol.*, 2008, **3**, 210.
58 B. Das, R. Voggu, C. S. Rout and C. N. R. Rao, *Chem. Commun.*, 2008, 5155.
59 R. Voggu, B. Das, C. S. Rout and C. N. R. Rao, *J. Phys.: Condensed Mater*, 2008, **20**, 472204.
60 O. Leenaerts, B. Partoens and F. M. Peeters, *Phys. Rev. B*, 2008, **77**, 125416.
61 S. Stankovich, D. A. Dikin, G. H. B. Dommett, K. M. Kohlhaas, E. J. Zimney, E. A. Stach, R. D. Piner, S. T. Nguyen and R. S. Ruoff, *Nature*, 2006, **442**, 282.
62 T. Ramanathan, A. A. Abdala, S. Stankovich, D. A. Dikin, M. H. Alonso, R. D. Piner, D. H. Adamson, H. C. Schniepp, X. Chen, R. S. Ruoff, S. T. Nguyen, I. A. Aksay, R. K. Prud'Homme and L. C. Brinson, *Nature Nanotechnol.*, 2008, **3**, 327.
63 B. Das, K. E. Prasad, U. Ramamurty and C. N. R. Rao, 2008, (communicated).

Published on 20 January 2009. Downloaded by IIT Jodhpur on 11/2/2023 9:13:43 PM.